CrossMark

ORIGINAL PAPER

Effects of U-ore on the chemical and isotopic composition of products of hydrous pyrolysis of organic matter

Yu-Wen Cai[1,2,3] · Shui-Chang Zhang[2,3] · Kun He[2,3] · Jing-Kui Mi[2,3] ·
Wen-Long Zhang[2,3] · Xiao-Mei Wang[2,3] · Hua-Jian Wang[2,3] · Chao-Dong Wu[1]

Abstract In order to investigate the impact of U-ore on organic matter maturation and isotopic fractionation, we designed hydrous pyrolysis experiments on Type-II kerogen samples, supposing that the water and water–mineral interaction play a role. U-ore was set as the variable for comparison. Meanwhile, anhydrous pyrolysis under the same conditions was carried out as the control experiments. The determination of liquid products indicates that the presence of water and minerals obviously enhanced the yields of C_{15+} and the amounts of hydrocarbon and non-hydrocarbon gases. Such results may be attributed to water-organic matter reaction in the high-temperature system, which can provide additional hydrogen and oxygen for the generation of gas and liquid products from organic matter. It is found that δD values of hydrocarbon gases generated in both hydrous pyrolysis experiments are much lower than those in anhydrous pyrolysis. What is more, δD values are lower in the hydrous pyrolysis with uranium ore. Therefore, we can infer that water-derived hydrogen played a significant role during the kerogen thermal evolution and the hydrocarbon generation in our experiments. Isotopic exchange was facilitated by the reversible equilibration between reaction intermediaries with hydrogen under hydrothermal conditions with uranium ore. Carbon isotopic fractionations of hydrocarbon gases were somehow affected by the presence of water and the uranium ore. The increased level of i-C_4/n-C_4 ratios for gas products in hydrous pyrolysis implied the carbocation mechanism for water-kerogen reactions.

1 Introduction

Organic and inorganic compounds coexist in most geological environments. Experimental and field studies have demonstrated that the presence of water, minerals and catalytically active transition metal elements in sedimentary basins can influence petroleum generation and accumulation (Goldstein 1983; Huizinga et al. 1987a, b; Pan et al. 2009, 2010; Tannenbaum and Kaplan 1985a, b; Mango 1992; Mango and Joe 1997). The classical hydrous pyrolysis system described by Lewan et al. had verified that many organic reactions cannot occur without water (Mayer 1994), which also plays an essential role in the process of petroleum generation, such as influencing the stability of crude oil and the secondary cracking of long-chain hydrocarbons (Lewan 1993, 1997). In addition, with increasing temperature, more chemical types of hydrogen in the organic matter become exchangeable with those in the water and result in isotopic shifts among kerogen, bitumen and oil, but only small changes in organic $^{13}C/^{12}C$ (Schimmelmann et al. 1999). Mineral catalysis has been suggested as an important factor in petroleum generation based on the catalytic activity of acidic clays during the refining process. Experiments using minerals ubiquitous in

✉ Shui-Chang Zhang
sczhang@petrochina.com.cn

1 School of Earth and Space Sciences, Peking University, Beijing 100087, China

2 Research Institute of Petroleum Exploration and Development (RIPED), Beijing 100083, China

3 State Key Laboratory of Enhanced Oil Recovery, Beijing 100083, China

 Springer

sedimentary basins as substrates, such as iron-bearing minerals, aluminum-containing minerals and silicates, suggested that these compounds might oxidize petroleum and generate organic acids and CO_2 (Seewald 2001, 2003; Seewald et al. 1998; Surdam et al. 1985, 1993). The minerals with catalytic activity, such as montmorillonite, that catalyze reactions under dry conditions, may also be inhibited by water (Tannenbaum and Kaplan 1985a).

Transition metal elements in source rocks have been pinpointed to be catalytic in the conversion of hydrogen and *n*-alkenes into natural gas. However, specific mechanisms remain equivocal (Mango 1992; Mango and Joe 1997; Lewan et al. 2008). Uranium, as a special transition metal element, has long been known to be associated with organic matter. Under reducing conditions, U(VI) is reduced to the immobile tetravalent state, U(IV), which mainly occurs in the organic-rich shales (Partin et al. 2013; Lev and Filer 2004; Lev et al. 2008; Fisher and Wignall 2001; Galindo et al. 2007). A lot of research has been carried out to investigate the role of organic components in metal mineralization, while the catalytic effects of uranium on oil cracking have rarely been studied or reported. Previous studies showed that U-bearing ore in source rocks acts as a catalyst, determining the degree, composition and timing of natural gas generation (Liu et al. 2006, 2013; Mao et al. 2012a, b, 2014; Li et al. 2008; Lu et al. 2007). This hypothesis may have important implications concerning gas generation in unconventional shale-gas accumulations. But since U-ore has a degree of radioactivity and serves as a complex catalyst under geological conditions, it is difficult to make breakthroughs in this field. Therefore, additional experiments are needed to better evaluate the significance of uranium in hydrocarbon generation from petroleum source rocks.

Based on oil cracking experiments in a confined pyrolysis system (gold tubes), we investigated the catalytic effects of U-ore on oil cracking, identified the chemical and isotopic features of gas hydrocarbons, and evaluated possible mechanisms in the system. Type-II kerogen samples with low maturity from the Xiamaling Formation were selected for isothermal anhydrous pyrolysis and hydrous pyrolysis under two conditions, with and without U-bearing ore.

2 Materials and methods

2.1 Samples

The kerogen samples used in our pyrolysis experiments were separated from the organic-rich immature source rocks from Xiamaling Formation, Xiahuayuan Area, Hebei Province, North China, with an age of 1384.4 ± 1.4 Ma (Zhang et al. 2015). The uranium ore was collected from a depth of 170 m below the surface of the Zoujiashan Deposit, Xiangshan Uranium Field, South China. Before pyrolysis, source rock samples were firstly crushed into powder (80–100 mesh), and then treated with solvents to obtain purified kerogen samples. The kerogen was isolated from the rocks by rinsing with HF/HCl, Soxhlet extraction for 72 h, washed with distilled water and dried at a low temperature (40 °C).

The geochemical features of the source rock, kerogen and minerals are listed in Table 1. The source rock has a TOC of 3.82%, hydrogen index (HI) of 369.09 mg/g TOC and T_{max} of 433 °C. The kerogen has an H/C ratio of 1.19 and an O/C ratio of 0.02, which is classified as Type-II kerogen. The U-bearing ore we used in the experiment is composed of 50% clay, 17.4% quartz, 26.1% fluorite and 6.6% feldspar, among which uranium mainly exists in the clay minerals, with the elemental content of 0.85% (Table 1).

2.2 Gold-tube pyrolysis

All pyrolysis experiments were performed in a gold-tube pyrolysis system at constant temperatures of 300, 330, 350, 360, 370, 390, 400 and 420 °C for time intervals between 24 and 360 h at a constant pressure of 50 MPa. These were carried out at the Petroleum Geology Research and Laboratory Center (PGRLC) of the Research Institute of Petroleum Exploration and Development (Zhang et al. 2013). The error for the temperature was less than ±1 °C. The tubes used in our experiments were 50 mm in length with an inner diameter (ID) of 4.0 mm and a wall thickness of 0.5 mm. The reactants were accurately measured and loaded into the tube. A series of anhydrous samples and two series of hydrous samples were loaded into the gold tubes. In anhydrous experiments, only 50 mg of kerogen samples were loaded, while in hydrous experiments samples were separated into two sets, one with kerogen plus 50 μg deionized water ($\delta D_{H2O} = -55‰$), and the other with the same amount of water and additional 50 mg of U-ore in order to magnify the impact of water and differentiate the effects of added minerals on the hydrocarbon generation. Air in the tube was removed by argon flow, and the other end of the tube was crimped and sealed by an argon arc welder with most of the sealed end submerged in liquid nitrogen. When reaction ended, the pressure was relieved, and the gold tubes were withdrawn. Before analysis, the tubes were weighed and compared with the preheated weight to determine whether leakage had occurred during pyrolysis.

After pyrolysis, the volatile components in the tubes were collected with a custom-made gas inlet device with a known volume. Prior to piercing a tube, the device was first evacuated to a pressure of less than 0.1 MPa, then gas was allowed to escape slowly into the evacuated inlet device, and

Table 1 Geochemical characteristics of the original samples and U-ore

Kerogen analyses		Whole rock analyses		Mineral and elemental analyses	
TOC wt%[a]	57.03	TOC wt%[a]	3.82	%Clay[c]	49.9
C%[b]	55.6	T_{max} (°C)[a]	433	%Fluorite[c]	26.1
Atomic H/C ratio[b]	1.19	S_1 (mg/g rock)[a]	2.12	%Quartz[c]	17.4
Atomic O/C ratio[b]	0.02	S_2 (mg/g rock)[a]	369.09	%Feldspar[c]	6.6
$\delta^{13}C$ (per mil, V PDB)	−33.2	S_3 (mg/g rock)[a]	1.11	%U[d]	0.85
δD (per mil, V SMOW)	−110.4	HI (mg S_2/g TOC)[a]	420	%Fe[d]	1.2
R_b%	0.5			%Al[d]	1.2

[a] Rock–Eval pyrolysis

[b] Elemental analyses

[c] X–ray diffraction

[d] ICP–MS analyses

the final pressure was recorded. The device was directly connected to a gas chromatograph (GC; 7890N, Agilent) to analyze the organic and inorganic gas compositions.

2.3 Product analyses

Qualitative and quantitative analysis of the individual hydrocarbon and non-hydrocarbon gas components were conducted by a two-channel Agilent 7890 Series Gas Chromatograph (GC) integrated with an auxiliary oven, which was custom configured by Wasson-ECE instrumentation (Fort Collins, CO). The instrument was fitted with two capillary and six packed analytical columns, a flame ionization detector (FID) and two thermal conductivity detectors (TCDs). The carrier gases for FID and TCD were high-purity N_2 and He, respectively. The temperature program of the GC oven was: heating from initial 68 °C (held for 7 min) to 90 °C (held for 1.5 min) at a rate of 10 °C/min, then to 175 °C (held for 5 min) at a rate of 15 °C/min. The analytical precision was ≤1 mol‰ (Zhang et al. 2007; He et al. 2011a).

Stable carbon isotopes ($\delta^{13}C$) were measured on the generated methane, ethane and propane gas with a GC/combustion/isotope ratio mass spectrometer (IRMS) (Finnigan MAT Delta, Thermo Fisher Scientific). Original stable carbon isotopes in the kerogen were determined by IRMS (Delta Plus V Advantage). Individual hydrocarbon components (C_{1-5}) and CO_2 were initially separated by using a chromatographic column. The chromatographic column temperature was increased from 35 to 80 °C at a rate of 8 °C/min, then to 260 °C at a rate of 5 °C/min, and the final oven temperature was held for 10 min. Each gas sample was analyzed twice, with an analytical precision of ±0.5‰ compared with the Vienna Pee Dee Belemnite (VPDB) standard.

The hydrogen isotopic (δD) analysis of the gases was performed by GC/thermal conversion/IRMS (Finnigan MAT 253 Delta). Gas components were separated by a chromatographic column, and helium was used as the carrier gas. Methane was injected in split mode (split ratio 1:7) with a constant temperature of 40 °C. Ethane was injected in splitless mode and was kept at an initial temperature of 40 °C for 4 min, heated to 80 °C at a rate of 10 °C/min, heated to 140 °C at a rate of 5 °C/min, and finally heated to 260 °C at a rate of 30 °C/min. The analytical precision was less than ±5‰.

Generated liquid products (C_{15+} compounds) were collected by dichloromethane (DCM) extraction of solid residues after pyrolysis. In a typical procedure, the gold tubes were cut in a glass bottle, weighed as G_0, with dichloromethane (DCM). The bottle was ultrasonicated twice for 3 min until the solvent and residues were totally separated. Then, we carefully filtered the solvent into another glass bottle, which was weighed as G_1, through the chromatographic membrane several times until the liquid was clean. After the volatilization of DCM in both two bottles, we weighed each glass bottle again, recorded as G_2 and G_3. The differences between G_2 and G_0 as well as G_3 and G_1 were due to C_{15+} compounds and solid residues after the pyrolysis, respectively (He et al. 2011a).

Total organic carbon (TOC) and rock evaluation analyses were conducted on the kerogen with a Rock–Eval 6 carbon analyzer. Elemental analyses (C, H, N and O) were determined with an elemental analyzer (vario MICRO cube, Elementar) using acetanilide as a standard for carbon, hydrogen and oxygen. Stable carbon isotope ratios of the residues were measured online with a combustion system (Flash EA–ConFlo IV, Thermo Fisher Scientific) connected to an isotope ratio mass spectrometer (IRMS; Delta Plus V Advantage, Thermo Fisher Scientific). $\delta^{13}C$ and δD values of kerogen were measured with a precision of ±0.5‰ and ±5‰, respectively. All $\delta^{13}C$ and δD values are reported in the permillage (‰) relative to Vienna Pee Dee Belemnite (VPDB) and Vienna Standard Mean Ocean Water (VSMOW), respectively. All the analyses were performed at the Petroleum Geology Research and Laboratory Center (PGRLC) of the Research Institute of Petroleum Exploration and Development.

Table 2 Detailed experimental conditions, yields, and carbon and hydrogen isotope ratios during pyrolysis of Type-II kerogen samples from the Xiamaling Formation at 50 MPa

Temp.,°C	Time, h	EasyR_o (%)	Total C_{15+} oils, mg/g TOC	Gas Yields (mL/g TOC)											C_1/C_{1-5}	iC_4/nC_4	Carbon isotope (‰, vs. VPDB)			Hydrogen isotope (‰, vs. VSMOW)		
				C_1	C_2	C_3	iC_4	nC_4	iC_5	nC_5	CO_2	H_2	H_2S	C_{2-5}			$\delta^{13}C_1$	$\delta^{13}C_2$	$\delta^{13}C_3$	δD_1	δD_2	δD_3
Kerogen																						
300	24	0.6	30.5	2.2	1	0.4	0	0.1	0	0	4.5	–	1.1	1.5	0.59	0.35	–51.9	–39.2	–39.7	–225	–146	–
	24	0.79	80.5	6.5	5.4	2.6	0.2	1.0	0.1	0.4	3.9	–	4.2	9.6	0.4	0.21	–51.5	–40.1	–38	–	–	–
330	72	0.89	136.8	12	10	6.1	0.6	3.1	0.3	1.2	4.3	–	6.2	21.3	0.37	0.2	–52.3	–39.7	–36.5	–236	–152	–156
	120	0.95	286.9	13.2	10.7	6.6	0.7	3.3	0.3	1.3	3.8	–	8.2	22.9	0.36	0.2	–52.3	–39.5	–36.7	–251	–168	–150
	240	1.05	523.2	19.4	14.1	8.3	0.8	4	0.3	1.5	3.5	–	10	29.1	0.4	0.21	–51.5	–38.3	–36.6	–252	–172	–142
350	120	1.17	403.7	26.2	15.8	9.2	1.0	4.3	0.4	1.5	4.4	–	12.4	32.1	0.45	0.23	–49.5	–37.6	–36	–254	–164	–121
	240	1.29	331.2	33	17.5	10.4	1.1	4.7	0.4	1.5	5.1	–	11.2	35.7	0.48	0.24	–48	–37.7	–36.6	–254	–162	–106
360	168	1.35	295.3	37.2	19.5	11.4	1.2	4.7	0.4	1.3	5.1	–	11.1	38.5	0.49	0.26	–48.3	–37.6	–36.1	–260	–161	–104
	240	1.42	225.1	41.3	19.8	11.7	1.4	5.1	0.5	1.6	5.7	–	11.7	40.1	0.51	0.27	–47.9	–37.5	–36.1	–254	–161	–102
370	168	1.49	179.3	46.6	21.6	13.3	1.6	5.8	0.5	1.8	5.7	–	11.3	44.7	0.51	0.28	–47	–36.7	–36	–255	–146	–95
	240	1.59	131.9	51.3	22.8	14.2	1.7	6	0.6	1.9	6.3	–	11.5	47.2	0.52	0.29	–47	–36.2	–36	–248	–138	–102
	360	1.66	92.2	68.5	16.5	16.4	1.7	5.3	0.6	1.7	8.1	–	10.3	42.2	0.62	0.32	–46.8	–37.5	–35.8	–	–	–
390	120	1.71	76.6	66.7	25.1	14.7	1.6	4.8	0.5	1.5	9.3	–	9.6	48.2	0.58	0.33	–46	–37.1	–34	–238	–	–
	168	1.8	69.9	71.5	29.4	18.2	2.2	6.3	0.7	1.9	10.8	0.1	10.9	58.8	0.55	0.35	–45.7	–36.7	–34.5	–232	–108	–95
	240	1.89	33.1	79	32.9	19.7	2.3	5.7	0.6	1.5	10.9	0.2	11.2	62.7	0.56	0.4	–45.4	–37	–34.5	–230	–96	–
	360	2.0	–	100.9	39.6	23.8	3.3	7.7	0.9	2.2	12.6	0.4	9.7	77.6	0.57	0.43	–45.3	–36.8	–34.1	–224	–83	–86
400	240	2.07	–	97.7	39.6	24.7	3.4	7.9	0.9	2	12	0.6	8.7	78.4	0.55	0.43	–44.9	–36.2	–33.6	–223	–90	–86
	360	2.19	–	110.7	43.5	26.6	4.2	8.7	0.8	1.7	12.9	0.8	10.3	85.5	0.56	0.49	–44.6	–36.1	–32.4	–212	–77	–81
420	168	2.35	–	134	47	24.1	3.3	5	0.3	0.6	13.3	1.4	10.4	80.4	0.62	0.65	–43.9	–35.4	–32.4	–185	–57	–56
	264	2.5	–	140.8	48	23.5	3.3	4.8	0.3	0.6	14.2	1.6	10.8	80.4	0.64	0.68	–42.3	–34.5	–29.3	–180	–29	–42
Kerogen plus deionized water and U-ore																						
300	24	0.6	67.8	5.8	2.2	1.2	0.2	0.3	0	0	1.6	–	0.1	3.9	0.6	0.92	–45.3	–35.6	–24.4	–	–	–
	24	0.79	137.2	5.7	2.2	0.9	0.1	0.2	0	0	5.1	–	0.1	3.4	0.63	0.65	–	–40.4	–	–	–	–
330	72	0.89	281.7	9.8	4.8	2.3	0.3	0.7	0	0	6.4	–	1	7.9	0.55	0.41	–46.6	–40	–36.2	–282	–233	–203
	120	0.95	354.1	13.3	6.6	3.2	0.4	1	0.1	0	7.2	–	0.5	11.2	0.54	0.43	–46.3	–39.7	–35.8	–286	–232	–204
	240	1.05	679.3	19.9	9.3	4.8	0.6	1.5	0.2	0	7.9	–	0.4	16.5	0.55	0.43	–46.8	–39.5	–35.7	–286	–217	–193
350	120	1.17	425.3	27.9	13.6	8.5	1.5	3.6	0.9	0.8	8.2	–	0.6	28.8	0.5	0.4	–48.4	–38.7	–34.9	–284	–208	–190
	240	1.29	304.2	38	16.9	10.3	1.8	4.4	1.1	1	8.1	–	0.6	35.5	0.52	0.42	–48.2	–37.7	–34.9	–282	–204	–188
360	168	1.35	221.9	41.5	18.2	11.6	2.1	5.1	1.2	1.1	8.7	–	0.5	39.2	0.51	0.41	–47.5	–37.5	–34.6	–280	–199	–180
	240	1.42	168.1	51.5	21.4	14	2.8	6.1	1.6	1.3	9.3	–	0.8	47.2	0.52	0.46	–47.1	–37.3	–34.3	–278	–200	–176
370	168	1.49	104.6	60.6	23.4	14.1	2.3	4.6	1.1	0.9	9.8	–	1.8	46.4	0.57	0.5	–46.8	–37.1	–34.1	–276	–181	–172
	240	1.59	102.9	70.9	26.7	16.9	3.2	6.3	0.1	1.5	11.5	0.4	2.5	54.7	0.56	0.51	–46.7	–37	–34	–272	–177	–166
	360	1.66	98.7	82.1	29.8	18.8	3.5	6.4	0.1	1.4	12.9	0.7	3.2	59.9	0.58	0.54	–45.3	–37.2	–34	–	–	–

Table 2 continued

Temp., °C	Time, h	EasyRo (%)	Total C$_{15+}$ oils, mg/g TOC	Gas Yields (mL/g TOC)											C$_1$/C$_{1-5}$	iC$_4$/nC$_4$	Carbon isotope (‰, vs. VPDB)			Hydrogen isotope (‰, vs. VSMOW)		
				C$_1$	C$_2$	C$_3$	iC$_4$	nC$_4$	iC$_5$	nC$_5$	CO$_2$	H$_2$	H$_2$S	C$_{2-5}$			δ^{13}C$_1$	δ^{13}C$_2$	δ^{13}C$_3$	δD$_1$	δD$_2$	δD$_3$
390	120	1.71	95.4	91	33	22	4.3	7.5	0.1	1.5	13.2	0.7	5.2	68.4	0.57	0.57	−45.2	−36.7	−33.6	−274	−168	−142
	168	1.8	85	103.2	36.2	24.3	5.1	8.7	0.1	1.7	14.2	1.1	5.3	76	0.58	0.59	−44.7	−36.4	−33.1	−272	−151	−146
	240	1.89	49.9	104.2	36.7	24.2	4.5	8.1	0.1	1.6	14.4	1.4	5.4	75.1	0.58	0.56	−44.9	−36.1	−33.7	−274	−137	−137
	360	2.0	–	130.4	44.5	31.6	8.1	12.1	0.1	1.9	15.3	1.6	8.5	82.3	0.57	0.67	−44	−36.1	−31.3	−268	−134	−126
400	240	2.07	–	140.3	42.7	29	6.3	9.4	0.1	1.5	19	2.2	10.6	89	0.61	0.67	−43.4	−35.7	−30.5	−264	−127	−131
	360	2.19	–	162.1	52.7	32	7.1	9.6	0.1	1.8	21.2	–	–	103.3	0.62	0.73	−42.8	−34.3	–	−251	–	–
420	168	2.35	–	185.3	53.5	33.1	7.9	10.2	1	0	–	3.5	–	104.9	0.61	0.87	−42.4	−33.7	−28	−235	−122	−128
	264	2.5	–	198.5	58.5	34.5	6.6	6.8	0.7	0.4	22.5	3.9	11.0	107.4	0.65	0.97	−40.9	−33.1	−27	−224	−112	−123
Kerogen plus deionized water																						
300	24	0.6	87.8	–	–	–	–	–	–	–	–	–	–	–	–	–	−41.4	–	–	–	–	–
	24	0.79	197.2	3.5	1.8	0.9	0.2	0.2	0	0.4	2.2	–	0.3	3.4	0.51	0.94	–	–	–	–	–	–
330	72	0.89	355	–	–	–	–	–	–	–	–	–	–	–	–	–	−45.6	−39.1	−37	−288	−219	−204
	120	0.95	510.2	8	3.7	1.7	0.3	0.4	0.1	0.1	4.5	–	0.7	6.2	0.56	0.78	−45.5	−39.8	−37.2	−286	−208	−196
	240	1.05	648.3	21.1	10.6	6.1	1.2	2.1	0.6	0.6	9.1	–	1.9	21.2	0.5	0.55	−45.4	−40	−38.2	−291	−209	−200
350	120	1.17	480.1	27.6	12.9	7.7	1.7	3	1.1	1	10.5	–	2.9	27.4	0.5	0.56	−45.8	−39.5	−37.8	−291	−202	−196
	240	1.29	332.9	41.6	17.8	11.2	2.6	4.5	1.7	1.4	11.3	–	4.6	39.3	0.51	0.58	−45.3	−39.2	−37.6	−284	−204	−179
360	168	1.35	256.2	47.2	19.9	13	3.2	5.2	2.1	1.5	11.6	–	5.7	45	0.51	0.62	−46	−38.4	−37.4	−274	−193	−160
	240	1.42	203	52.6	21.3	14	3.3	5.5	2.1	1.5	12.2	–	5.3	47.6	0.52	0.6	−46	−38.6	−37.6	−276	−188	−164
370	168	1.49	133.6	61.7	24.3	16.3	4.1	6.3	2.6	1.8	13.5	0.5	6.8	55.4	0.53	0.64	−45.7	−38.2	−37.2	−280	−176	−157
	240	1.59	91.2	78	29	20.6	5.7	8.3	3.9	2.5	14.3	0.7	8.9	70	0.53	0.68	−44.6	−37.4	−36.9	−274	−169	−145
	360	1.66	42.4	85.8	31	22	6.3	8.2	0.1	2.1	15.4	0.9	13.8	69.8	0.55	0.77	−44.2	−37.9	−36.9	−277	−147	−128
390	120	1.71	–	87.4	32	23.6	6.7	9.5	4.5	2.6	16.9	1.4	16.5	78.9	0.53	0.7	−43.9	−37.6	−36.7	−261	−148	−130
	168	1.8	–	94.9	34.5	25.5	7.2	9.5	4.2	2.2	18.4	1.4	17.5	83	0.53	0.76	−44	−37.4	−36	−257	−126	−121
	240	1.89	–	103.2	34.9	24.7	6.8	9.3	4	2.4	20.1	1.5	19.7	82.2	0.56	0.73	−43.6	−37.4	−36	−250	−113	−116
	360	2.0	–	124.3	40.8	29.2	8.7	9.8	3.6	1.8	22.8	2	20.4	93.9	0.57	0.89	−42.7	−37.2	−35.7	−240	−106	−103
400	240	2.07	–	132.8	43	30.5	8.6	9.9	0.1	1.8	27.1	2.8	23.6	93.9	0.59	0.87	−43.1	−37	−34.4	−235	−103	−101
	360	2.19	–	133.8	42.6	30.7	8.9	10	3.2	1.7	27.6	3.2	25.4	97.2	0.58	0.89	−43.2	−36.8	−33.3	−226	−99	−100
420	168	2.35	–	148.5	45.1	30.8	7.7	8.8	1.9	1.1	27.9	3.6	27.3	95.5	0.61	0.88	−42.5	−36.4	−34	−221	−95	−104
	264	2.5	–	159.3	45.7	31.4	8.3	8.6	1.9	1	28.2	3.6	26.4	96.8	0.62	0.96	−42.4	−36	−33.1	−211	−95	−98

EasyRo % values were calculated in Matlab according to Sweeney and Burnham (1990)

The amounts of kerogen, uranium ore and deionized water were 50 mg, 50 mg and 50 μL, respectively

– not detected
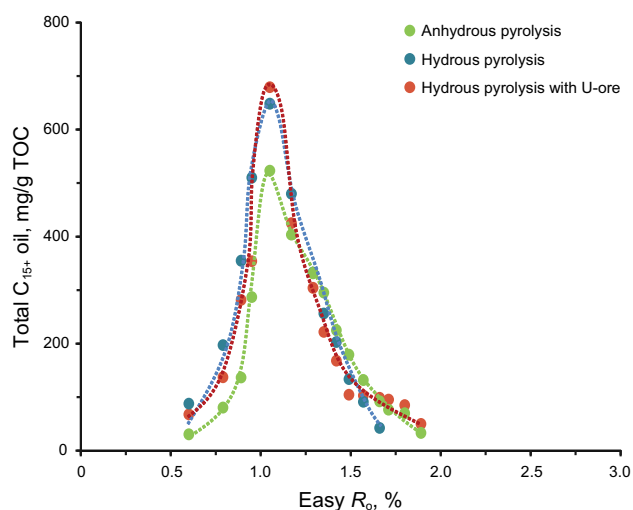
Fig. 1 Yields of total C_{15+} oils versus $EasyR_o\%$ of kerogen generated under conditions of no added water (*green points*), added water (*blue points*), and added water plus U-ore (*red points*)

3 Results

3.1 Yields of C_{15+} oils

After heating for 1, 3, 5, 7, 10 and 15 days at different temperatures, equivalent R_o values ($EasyR_o\%$ using the Sweeney and Burnham (Sweeney and Burnham 1990) kinetic model to estimate maturity) were calculated, ranging from 0.6% to 2.5% (Table 2).

Total C_{15+} oils from anhydrous and hydrous experiments were given relative to TOC (mg/g) and $EasyR_o\%$ (normalized percentage) (Table 2; Fig. 1). As demonstrated in Fig. 1, all three experiments show a similar trend concerning the relationship between temperature and $EasyR_o\%$. In anhydrous and hydrous experiments with and without uranium ore, yields of C_{15+} oils at first increased rapidly from the initial values, 30.5, 67.8 and 87.8 mg/g TOC, to the maximum values, 523.2, 679.3 and 648.3 mg/g TOC with an $EasyR_o$ of 1.05%, and then decreased with further increased heating time. Experiments with water produced more oil than those without water, and the hydrous experiments with added U-ore produced more oil as well. Obviously, the presence of water and U-ore apparently enhanced oil yields from Type-II kerogen on different levels. Nevertheless, oil generation peaks were not affected in terms of the same $EasyR_o\%$ (Fig. 1).

3.2 Yields of gas products

The amounts and ratios of gas compositions produced during experiments are shown in Table 2 and Fig. 2. The amounts of generated methane decrease in the order of

hydrous experiments with added uranium ore (5.8–198.5 mL/g TOC), those without uranium ore (3.5–159.3 mL/g TOC), and those without water and U-ore (2.2–140.8 mL/g TOC) (Fig. 2a).

In contrast to the continuously increasing yields of methane, the yields of wet gases (C_{2-5}) first increased to maximum values and then barely changed (Fig. 2b). Maximum values are 107.4 mL/g TOC, 96.8 mL/g TOC and 80.4 mL/g TOC for the kerogen pyrolysis under conditions with water plus uranium ore, with water, and without water, respectively.

Among non-hydrocarbon gases, CO_2 is the most abundant, followed by H_2S (Table 2). The yields of CO_2 generated from pyrolysis with added water generally exceeded those without water. As shown in Fig. 2c, hydrous experiments with U-ore produced less CO_2 than those without U-ore, ranging from 1.6 to 22.5 mL/g TOC, and 2.2 to 28.2 mL/g TOC, respectively.

The yields of H_2S show different trends compared with those of CO_2. For anhydrous experiments, the yields of H_2S increased from 1.1 to 10.8 mL/g TOC before $EasyR_o\%$ reached 1%, and then the yields remained unchanged with increasing temperature and $EasyR_o\%$. On the contrary, in both hydrous experiments, the yields of H_2S were substantially lower when $EasyR_o\%$ was less than 1.5%, especially in the experiments with uranium ore. When $EasyR_o\%$ is larger than 1.5%, yields of hydrous experiments without uranium ore (8.9–26.4 mL/g TOC) exceeded those of anhydrous experiments. Meanwhile, the yields of experiments with U-ore gradually increased, but were still lower than those of the anhydrous pyrolysis. The phenomenon may be due to H_2S being removed by dissolution in water, and rapid reaction with the iron or uranium contained in the mineral assemblage to form pyrrhotite ($Fe_{1-x}S$) (Lewan 1993). Both hydrous pyrolysis tests displayed a very similar evolution pattern in terms of the yields of H_2 (Table 2; Fig. 2d). The values increased from the initial value of 0.4 mL/g TOC ($EasyR_o\% = 1.59\%$) to 3.9 mL/g TOC ($EasyR_o\% = 2.5\%$). They are substantially higher than those in anhydrous experiments, with the values from 0.1 mL/g TOC ($EasyR_o\% = 1.8\%$) to 1.6 mL/g TOC ($EasyR_o\% = 2.5\%$).

For the three experiments, the C_1/C_{1-5} ratios first decreased to minimum values in the $EasyR_o\%$ range of 0.6%–1.2%, and then increased consistently with temperature and $EasyR_o\%$. Under conditions with lower $EasyR_o\%$, hydrocarbons with longer alkyl chains including C_{15+} oils and C_{2-5} were dominant products. As temperature increased, the early generated oils and the methyl bonded in kerogen structures were cracked to generate more methane. The minimum values are 0.36 ($R_o = 0.95\%$), 0.50 ($R_o = 1.05\%$) and 0.50 ($R_o = 1.17\%$) in the experiments under conditions with exclusive kerogen, kerogen
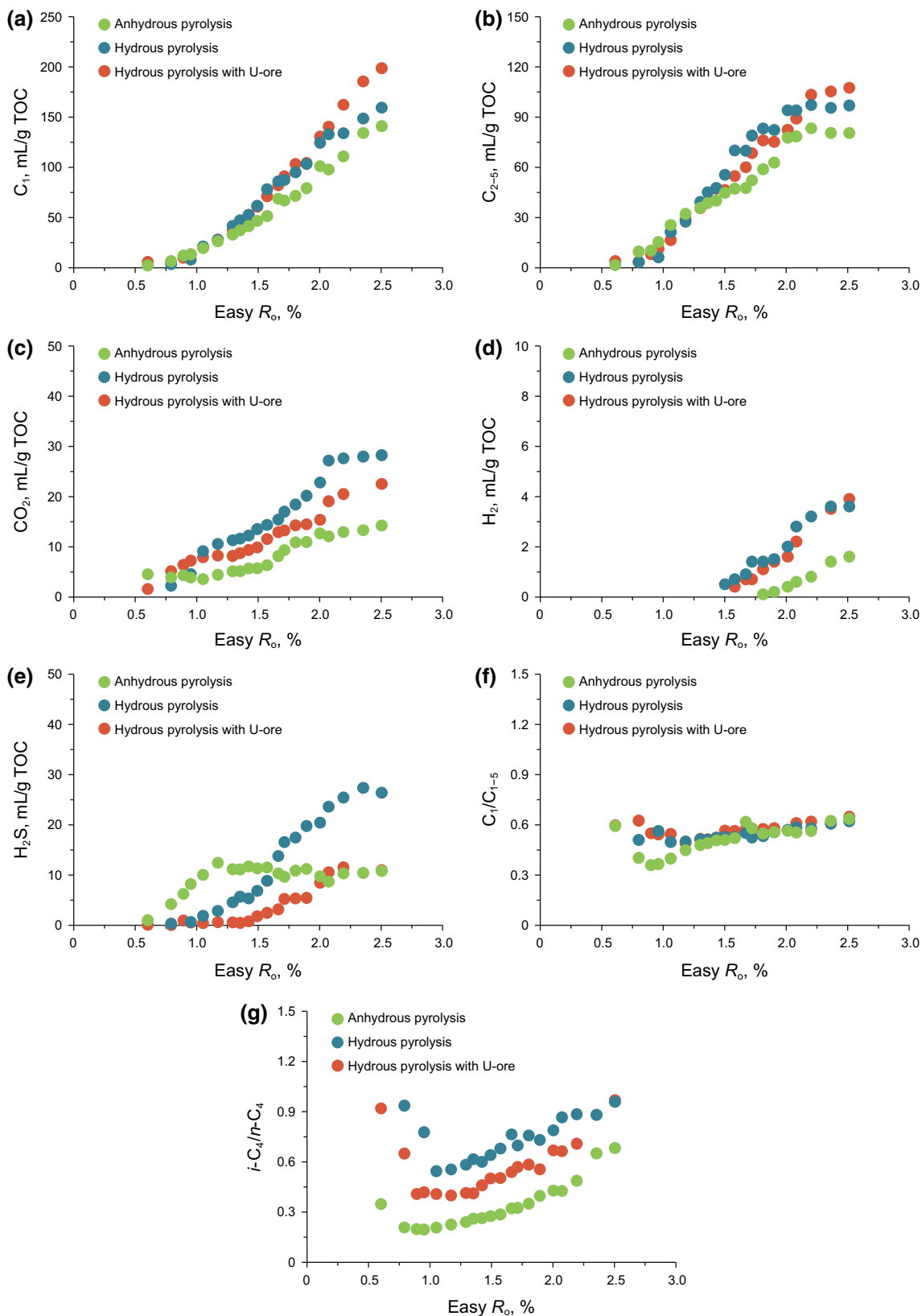
Fig. 2 Yields of **a** methane, **b** wet gases (C_{2-5}), **c** CO_2, **d** H_2, **e** H_2S, **f** C_1/C_{1-5} and **g** i-C_4/n-C_4 of kerogen generated under conditions with no added water (*green points*), added water (*blue points*), and added water plus U-ore (*red points*)
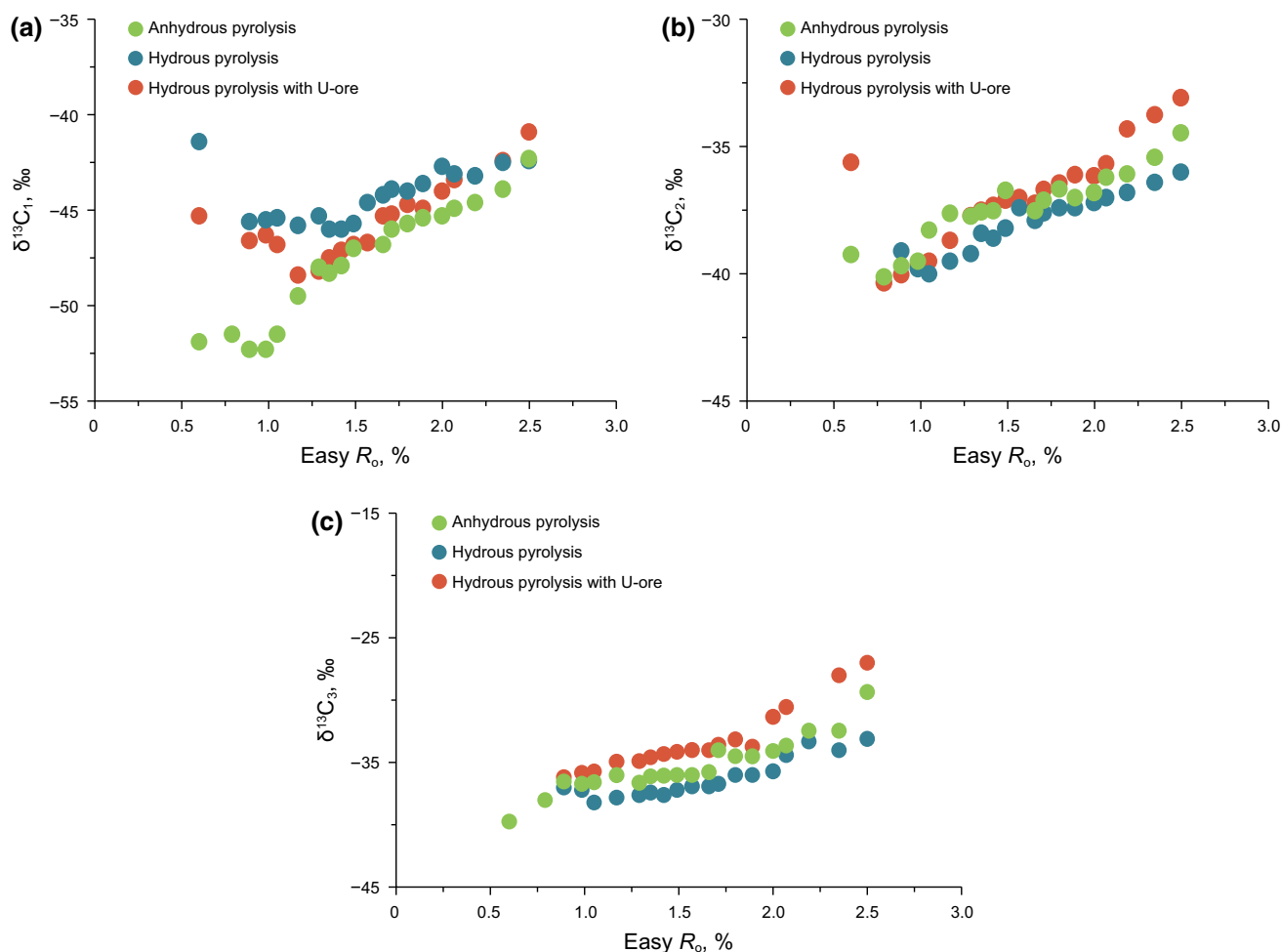
Fig. 3 Carbon isotopic compositions of **a** methane, **b** ethane, and **c** propane of kerogen generated under conditions with no added water (*green points*), added water (*blue points*), and added water plus U-ore (*red points*)

plus water, kerogen plus water and uranium ore, which corresponded closely to the maximum values of total C_{15+} oils (Table 2). This was also observed in previous experimental studies on Type-I and Type-II kerogens (Lorant et al. 1998; Pan et al. 2009).

The trends of the $i\text{-}C_4/n\text{-}C_4$ ratios for kerogen without water are relatively lower than those with water. For the ratios in anhydrous and hydrous pyrolysis with and without uranium ore, the values first decreased rapidly from high values of 0.35, 0.92 and 0.94 to the lowest values, 0.2, 0.4 and 0.58, and then increased again to 0.68, 0.97 and 0.96.

3.3 Carbon and hydrogen isotopes of hydrocarbon gases

3.3.1 Carbon isotopes

Stable carbon and hydrogen isotope ratios of produced hydrocarbon gases during thermal cracking of kerogen under controlled hydrous laboratory conditions are useful

to correlate characteristic isotopic responses with differences in source materials and experimental conditions. The carbon isotope compositions of methane, ethane and propane are shown in Table 2 and Fig. 3. The $\delta^{13}C$ values of methane ($\delta^{13}C_1$) became more negative with the $EasyR_o\%$ of about 0.95% in all the experiments. The lowest values are –52.3, –48.4 and –46.0‰ for the pyrolysis of exclusive kerogen, kerogen plus water and kerogen plus water and U-ore (Table 2; Fig. 3a). After the minimum values were reached, all the experiments showed consistent monotonic $\delta^{13}C_1$ enrichment with increasing maturity, ranging from –52.3 to –41.5‰ for anhydrous experiments, and from –46 to –40.9‰, from –48.4 to –42.4‰ for hydrous experiments with and without uranium ore, respectively. The $\delta^{13}C$ values of ethane ($\delta^{13}C_2$) showed the same trends with $\delta^{13}C_1$. The minimum values are –39.7, –38.2 and –36.2‰ in the $EasyR_o\%$ interval of 0.95–1.14% for the anhydrous experiments and hydrous experiments without and with uranium ore, and all the values increased to about –30.0 ± 3‰ (Fig. 3b). The trends of $\delta^{13}C$ value of propane
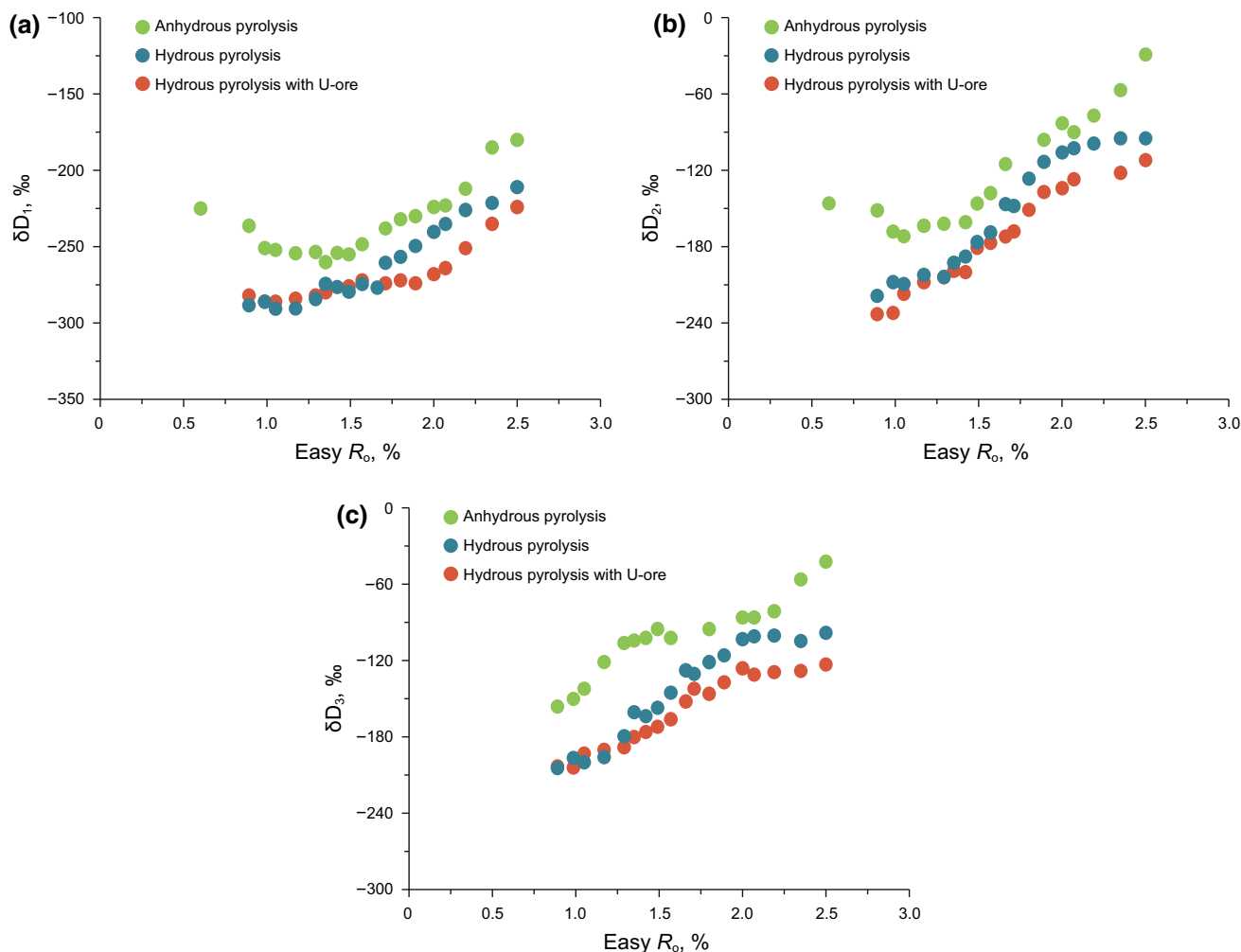
Fig. 4 Hydrogen isotopic compositions of **a** methane, **b** ethane, and **c** propane from kerogen generated under conditions with no added water (*green points*), added water (*blue points*), and added water plus U-ore (*red points*)

($\delta^{13}C_3$) are similar at the same temperature among all the sequences, with isotopic differences ranging between about –39.7 and –28.4‰ (Fig. 3c). And within all the experiments, $\delta^{13}C_1$ values are always more negative than the corresponding $\delta^{13}C$ values of ethane ($\delta^{13}C_2$) and propane ($\delta^{13}C_3$).

3.3.2 Hydrogen isotopes

The δD trends in the three experiments are shown in Table 2 and Fig. 4. In contrast to the carbon isotope compositions, the δD values for the hydrous experiments are less negative than those for the anhydrous experiments. In the experiments without water, δD values of methane (δD_1) range from –260 to –180‰. In the experiments with water and water plus uranium ore, δD values of methane (δD_1) range from –291 to –211‰ and from –286 to –224‰, respectively, with increasing temperature and

EasyR_o. δD values of ethane (δD_2) and propane (δD_3) also show consistent enrichment throughout pyrolysis, for hydrous experiments without uranium ore, and the values are between –219 and –95‰, and –204 and –98‰, respectively. For hydrous experiments with uranium ore, the value ranges are –233 to –112‰ and −203 to –123‰. And in anhydrous pyrolysis, the value ranges are −172 to –29‰, and −156 to –42‰ (Table 2).

3.4 Isotopic compositions and elemental ratios of residues

3.4.1 Elemental ratios of residues

The isotopic compositions of residues and elemental ratios obtained from anhydrous and hydrous pyrolysis experiments are presented in Table 3 and Fig. 5. The effect of increasing thermal maturation and consequent conversion of kerogen into oil and gas was indicated by the decrease in

Table 3 Isotopic and elemental ratios of the residues during anhydrous and hydrous pyrolysis with and without U-ore

Temp., °C	Time, h	EasyR_o (%)	Carbon isotopes (‰, vs. VPDB)	Hydrogen isotopes (‰, vs. VSMOW)	Elemental ratios	
					H/C	O/C
Anhydrous condition						
300	24	0.6	−33.4	−110.9	1.06	0.01
	24	0.79	−33.9	−104.1	0.90	0.02
330	72	0.89	−33.3	−93.0	0.76	0.03
	120	0.95	−33.4	−89.5	0.72	0.04
	240	1.05	−33.3	−89.8	0.61	0.02
350	120	1.17	−33.4	−87.8	0.58	0.02
	240	1.29	−33.2	−85.4	0.55	0.02
360	168	1.35	−33.2	−87.6	0.59	0.02
	240	1.42	−33.3	−88.6	0.55	0.02
370	168	1.49	−33.0	−88.4	0.52	0.02
	240	1.59	−33.0	−88.9	0.51	0.02
	360	1.66	−32.9	−89.4	0.51	0.02
390	120	1.71	−32.9	−87.8	0.50	0.02
	168	1.8	−33.0	−87.5	0.51	0.02
	240	1.89	−33.1	−87.2	0.50	0.01
	360	2.0	−32.9	−85.9	0.47	0.01
400	240	2.07	−33.1	−86.0	0.48	0.02
	360	2.19	−33.0	−83.7	0.46	0.02
420	168	2.35	−33.0	−81.9	0.46	0.02
	264	2.5	−33.0	−77.6	0.44	0.02
Kerogen plus deionized water and U–ore						
300	24	0.6	−33.4	−108.1	1.23	0.08
	24	0.79	−32.8	−109.3	1.13	0.11
330	72	0.89	−33.3	−111.7	1.04	0.11
	120	0.95	−33.3	−112.2	1.02	0.12
	240	1.05	−32.9	−104.6	0.82	0.10
350	120	1.17	−33.2	−104.7	0.87	0.12
	240	1.29	−33.4	−107.2	0.79	0.12
360	168	1.35	−33.3	−103.2	0.84	0.09
	240	1.42	−33.4	−104.4	0.76	0.12
370	168	1.49	−33.3	−106.2	0.68	0.10
	240	1.59	−33.3	−105.1	0.64	0.08
	360	1.66	−33.3	−107.4	0.64	0.08
390	120	1.71	−33.3	−106.3	0.58	0.06
	168	1.8	−33.2	−103.4	0.61	0.09
	240	1.89	−33.2	−101.5	0.66	0.09
	360	2.0	−33.1	−102.3	0.58	0.05
400	240	2.07	−33.2	−108.0	0.56	0.07
	360	2.19	−33.2	−106.3	0.56	0.05
420	168	2.35	−33.1	−106.5	0.55	0.05
	264	2.5	−33.1	−104.8	0.53	0.06
Kerogen plus deionized water						
300	24	0.6	−33.5	−122.4	1.14	0.02
	24	0.79	−33.4	−129.7	1.04	0.02
330	72	0.89	−33.3	−130.1	0.95	0.02

Table 3 continued

Temp., °C	Time, h	EasyR_o (%)	Carbon isotopes (‰, vs. VPDB)	Hydrogen isotopes (‰, vs. VSMOW)	Elemental ratios	
					H/C	O/C
	120	0.95	−33.2	−128.5	0.89	0.03
	240	1.05	−33.3	−127.4	0.83	0.04
350	120	1.17	−33.3	−126.0	0.67	0.05
	240	1.29	−33.2	−127.7	0.62	0.05
360	168	1.35	−33.2	−120.6	0.60	0.05
	240	1.42	−33.1	−126.4	0.59	0.04
370	168	1.49	−33.3	−129.3	0.55	0.04
	240	1.59	−33.4	−135.0	0.53	0.04
	360	1.66	−33.4	−129.5	0.53	0.04
390	120	1.71	−33.4	−132.8	0.51	0.05
	168	1.8	−33.4	−135.8	0.55	0.04
	240	1.89	−33.4	−137.2	0.53	0.04
	360	2.0	−33.3	−134.3	0.47	0.05
400	240	2.07	−33.4	−131.4	0.47	0.06
	360	2.19	−33.5	−132.5	0.49	0.05
420	168	2.35	−33.4	−134.1	0.45	0.05
	264	2.5	−33.5	−144.1	0.47	0.05

atomic H/C and O/C ratios in both experiments (Table 3; Fig. 5a, b). These geochemical parameters decreased with increasing maturity, as a result of losing hydrogen and carbon during the oil and gas generation and expulsion. Compared with the anhydrous experiments, the hydrous experiments showed a considerable increase in elemental atomic ratios (H/C and O/C), and the ratios of hydrous pyrolysis generally exceeded those from the experiments with no water added. In the hydrous experiments, the ratios of H/C ranged from 1.23 to 0.53 for experiments with added U-ore and from 1.14 to 0.47 for experiments without added U-ore. The ratios of O/C were 0.08 to 0.06 and 0.02 to 0.05 for experiments with and without U-ore. In the anhydrous experiments, the H/C ratios were 1.06 to 0.44, while O/C ratios were 0.01 to 0.02 (Fig. 5a). This result implies that both hydrogen and oxygen were incorporated during pyrolysis, which is consistent with the higher amount of CO_2 produced in the hydrous experiments (Table 2).

3.4.2 Isotopic compositions of residues

Changes in the carbon isotope compositions of the residues ($\delta^{13}C_{residues}$) show similar trends with those of the gases in Sect. 3.3 (Fig. 3), generally ranging from −33.4 to −33‰ for the three experiments (Table 3; Fig. 5c). All hydrogen isotope ratios of the residues ($\delta D_{residues}$) from the pyrolysis experiments with added water were significantly more negative than those without water (Table 3; Fig. 5d), which

are consistent with the notably lower values of δD in the gases produced in the hydrous experiments (Fig. 4). However, δD values of hydrous experiments with added uranium ore range from −108.1 to −104.8‰, which are higher than those without uranium ore, with the values between −130.1 and −144.1‰.

4 Discussion

The apparent increase in liquid and gas products, as well as the depletion of deuterium in hydrocarbon gases in hydrous pyrolysis, demonstrated that water and uranium ore could participate in the thermal evolution of organic matter and provide hydrogen for hydrocarbon generation. Indeed, previous experimental work by Lewan (1997) found that water plays a positive role in the generation of oil from organic matter. Liquid water can act as an exogenous hydrogen source that inhibits cross-link reactions during anhydrous pyrolysis and promotes hydropyrolysis by free-radical reactions or carbocation reactions (Lewan 1997; He et al. 2011b). Moreover, the increase in H_2, the slowly decreasing H/C ratios, and the lower δD values of solid residues or kerogen during hydrous pyrolysis also demonstrated that water and mineral-derived hydrogen have been introduced, which reacted with kerogen (Hoering 1984; Leif and Simoneit 2000; Lewan 1997; Schimmelmann et al. 1999). Hence, water and uranium ore were critical in the generation of oil and
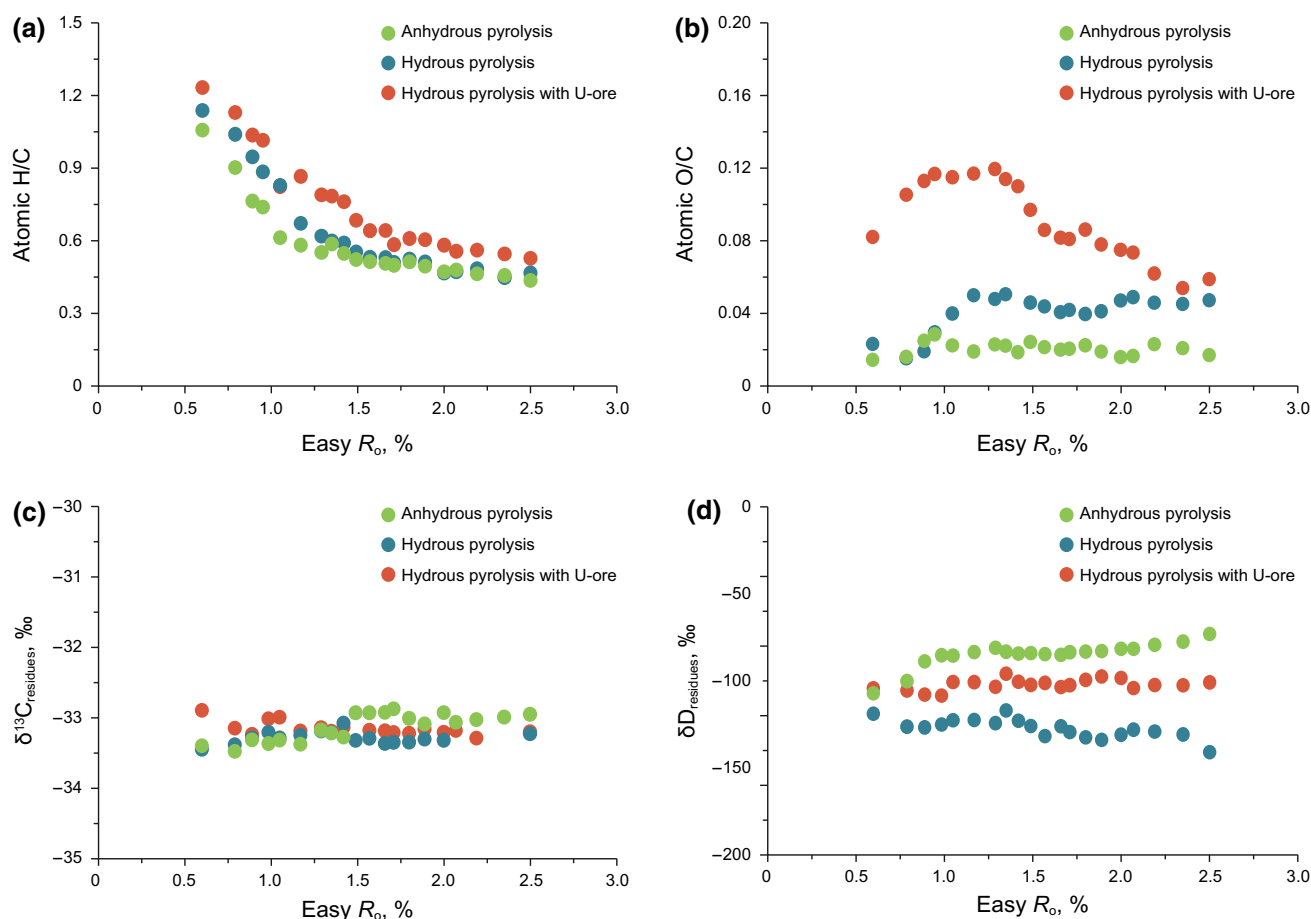
Fig. 5 Isotopic and elemental ratios of **a** H/C, **b** O/C, **c** $\delta^{13}C_{residues}$, and **d** $\delta D_{residues}$ of kerogen generated under conditions with no added water (*green points*), added water (*blue points*), and added water plus U-ore (*red points*)

gas as well as the thermal evolution of kerogen matter in our pyrolysis. Meanwhile, the mechanisms in the two tests of hydrous pyrolysis may differ a lot compared with that for kerogen cracking under anhydrous conditions. As is known, the generation of normal alkanes and isomeric alkanes during the cracking of organic compounds usually reflects free-radical reactions and carbocation reactions, respectively (Johns 2003; Kissin 1987). As shown in Table 2 and Fig. 2, the i-C_4/n-C_4 ratios for gas products were evidently higher in the hydrous experiments than those in anhydrous experiments. Such results demonstrated that the carboncation mechanism which was induced by the H^+ dissociated from the water should be presented (Siskin and Katritzky 1991; Leif and Simoneit 2000; Seewald 2001; Kissin 1987). What is more, the i-C_4/n-C_4 ratios in the hydrous experiments for kerogen plus U-ore were consistently lower compared with those without added U-ore, which is somehow opposite to the increased ratios in the previous study on kerogen with added clay mineral and water (Sweeney and Burnham 1990; Pan et al. 2010). The results indicated that the presence of U-ore inhibited the carbocation mechanism.

However, the increased yields of oil and gas implied there should be another reaction mechanism dominating hydrogenation during the hydrous pyrolysis with carbocations.

Additional insights into the difference among the three experiments were obtained from the isotopic data. The presence of added water with an initial $\delta D = -55‰$ caused about 20‰ deuterium-depletion in methane, which indicated that the isotopic transfer of water hydrogen into methane was affected by a kinetic fractionation favoring ^1H (Schimmelmann et al. 1999). Hydrogen atoms from organic compounds and other available hydrogen atoms, including those from water, might participate in thermal maturation. The transfer between water-derived hydrogen and organic compound-derived hydrogen had been observed in several studies using D_2O (Hoering 1984; Leif and Simoneit 2000; Lewan 1997) and deuterium-enriched water (Schimmelmann et al. 1999) under artificial thermal maturation conditions. The hydrogen transfer mechanisms that rely on the activation energy of various organic moieties vary. For example, in organic compounds, hydrogen bound to O, N or S can easily react with water vapor at low

temperature. Hydrogens connected to C=O and COOH, or in condensed aromatic systems, are exchangeable at elevated temperatures and suitable pH via enolization. Alkyl hydrogens are non-exchangeable owing to the strong, nonpolar covalent bond to carbon (Sessions et al. 2004). Similar trends in isotopic exchange were also observed in $\delta^{13}C_1$. In the pyrolysis experiments, $\delta^{13}C_1$ initially decreased from a high value to a minimum value, and then increased with temperature and EasyR_o. This reversal implies that carbon cracking changed from labile bonds (between carbon and heteroatoms) to C–C bonds (Cramer 2004), and this observation is consistent with many previous studies (Liu et al. 2004; Lorant et al. 1998; Tang et al. 2000; Tian et al. 2012; Xiao et al. 2005; Xiong et al. 2004). All pyrolysis experiments were conducted under the same pressure, excluding the possibility of varying isotopic fractionation during gas generation and expulsion under different pressures.

As shown in Fig. 4 and Table 2, a higher depletion of hydrogen isotopic compositions of the gas products was observed in the hydrous pyrolysis with added U-ore than those without uranium ore, and the isotopic change accelerated with increasing temperature. This difference might be most readily interpreted by the different reaction pathways between organic matter and water. In hydrous pyrolysis without the uranium ore, hydrogen from water simply exchanged with organic matter through a carbocation mechanism or by direct addition to the double bonds in the pyrolysis (Lewan 1997; Schimmelmann et al. 1999). However, in the experiments with uranium ore, more complex mechanisms might be involved, and water could at first react with minerals during the pyrolysis to produce hydrogen gas (Seewald 2001, 2003), and the latter would continually react with kerogen to produce hydrocarbon. The secondary-fractionation of hydrogen caused the values of δD_{H2} to be relatively lower than the values of water or organic matter, and further affected the hydrogen isotope ratio of products (Schimmelmann et al. 1999; Seewald 2001; Leif and Simoneit 2000). Furthermore, as proposed by Seewald (2001, 2003), in the conditions with water and U-ore the aqueous n-alkanes decomposed through a series of oxidation and hydration reactions, which produced reaction intermediaries, including alkenes, alcohols, ketones and organic acids. The chemical changes during the pyrolysis would affect the exchangeability of hydrogen atoms. For example, a hydrogen atom adjacent to electron-withdrawing groups, such as carbonyl, carboxyl, alcohol or amino groups, can exchange with ambient water over relatively short geologic timescales (Seewald 2001; Larcher et al. 1986). Thus, the attainment of this rapidly reversible metastable thermodynamic equilibrium provided a pathway for hydrogen exchange and enhanced the exchange rates (Reeves et al. 2012).

5 Conclusions

In this study, we compared the chemical and isotopic compositions of thermogenic gas and oil generated during pyrolysis of Type-II kerogen with variation of EasyR_o%, an index reflecting maturity, from 0.6% to 2.5%. Pyrolysis experiments were carried out in the presence and absence of water and U-ore in sealed gold tubes under different conditions with eight temperatures ranging from 300 to 420 °C. The conclusions are as follows:

1. In the hydrous experiments with and without U-ore, the yields of C_{15+} oils increased from 67.8 mg/g TOC and 87.8 mg/g TOC to 679.3 mg/g TOC and 648.3 mg/g TOC, respectively, which are 29% higher than those of anhydrous pyrolysis. Amounts of gas products, including methane, ethane, CO_2 and H_2 also increased to different degrees. The results demonstrated that water and U-ore provided sources of hydrogen and oxygen in the hydrocarbon generation.
2. The gas products and residues of hydrous pyrolysis were deuterium-depleted, and the residues had a higher elemental atomic ratio than the anhydrous pyrolysis counterparts, which suggested that water-derived hydrogen and oxygen, as well as uranium ore derived oxygen were incorporated into the gas products of hydrous pyrolysis, and were exchanged with the kerogen during the process. The δD values of the gas products were much lower in hydrous pyrolysis with uranium ore, indicating that the generation of H_2 occurred in hydrous pyrolysis with U-ore, which accounts for the higher depletion of deuterium in the gas products.
3. The main reaction in the pyrolysis of kerogen with water is the carbocation mechanism, reflected by a higher ratio of i-C_4/n-C_4 in the hydrous pyrolysis than that in the anhydrous pyrolysis. The lower i-C_4/n-C_4 ratios of the hydrous experiments plus U-ore indicated that the carbocation mechanism was inhibited to some extent.

References

Cramer B. Methane generation from coal during open system pyrolysis investigated by isotope specific, Gaussian distributed

reaction kinetics. Org Geochem. 2004;35(4):379–92. doi:10.1016/j.orggeochem.2004.01.004.

Fisher QJ, Wignall PB. Palaeoenvironmental controls on the uranium distribution in an Upper Carboniferous black shale (Gastrioceras listeri, Marine Band) and associated strata England. Chem Geol. 2001;175(3):605–21. doi:10.1016/S0009-2541(00)00376-4.

Galindo C, Mougin L, Fakhi S, et al. Distribution of naturally occurring radionuclides (U, Th) in Timahdit black shale (Morocco). J Environ Radioact. 2007;92(1):41–54. doi:10.1016/j.jenvrad.2006.09.005.

Goldstein TP. Geocatalytic reactions in formation and maturation of petroleum. AAPG Bull. 1983;67(1):52–159. doi:10.1306/03b5acd7-16d1-11d7-8645000102c1865d.

He K, Zhang SC, Mi JK. Research on the kinetics and controlling factors for oil cracking. Nat Gas Geosci. 2011a;22(02):211–8. doi:10.11764/j.issn.1672-1926.2011.02.211 **(in Chinese)**.

He K, Zhang S, Mi J, et al. Mechanism of catalytic hydropyrolysis of sedimentary organic matter with MoS_2. Pet Sci. 2011b;08(2):134–42. doi:10.1007/s12182-011-0126-0.

Hoering TC. Thermal reactions of kerogen with added water, heavy water and pure organic substances. Org Geochem. 1984;5(4):267–78. doi:10.1016/0146-6380(84)90014-7.

Huizinga BJ, Tannenbaum E, Kaplan IR. The role of minerals in the thermal alteration of organic matter-III. Generation of bitumen in laboratory experiments. Org Geochem. 1987a;11(6):591–604. doi:10.1016/0016-7037(85)90128-0.

Huizinga BJ, Tannenbaum E, Kaplan IR. The role of minerals in the thermal alteration of organic matter-IV. Generation of n-alkanes, acyclic isoprenoids, and alkenes in laboratory experiments. Geochim Cosmochim Acta. 1987b;1(5):1083–97. doi:10.1016/0016-7037(85)90128-0.

Johns WD. Clay mineral catalysis and petroleum generation. Annu Rev Earth Planet Sci. 2003;7(1):183–98. doi:10.1146/annurev.ea.07.050179.001151.

Kissin YV. Catagenesis and composition of petroleum: origin of n-alkanes and isoalkanes in petroleum crudes. Geochim Cosmochim Acta. 1987;51(9):2445–57. doi:10.1016/0016-7037(87)90296-1.

Larcher AV, Alexander R, Rowland SJ, et al. Acid catalysis of alkyl hydrogen exchange and configurational isomerisation reactions: acyclic isoprenoid acids. Org Geochem. 1986;10(4–6):1015–21. doi:10.1016/S0146-6380(86)80040-7.

Leif RN, Simoneit BRT. The role of alkenes produced during hydrous pyrolysis of a shale. Org Geochem. 2000;31(11):1189–208. doi:10.1016/S0146-6380(00)00113-3.

Lev SM, Filer JK. Assessing the impact of black shale processes on REE and the U–Pb isotope system in the southern Appalachian Basin. Chem Geol. 2004;206(3):393–406. doi:10.1016/j.chemgeo.2003.12.012.

Lev SM, Filer JK, Tomascak P. Orogenesis vs. diagenesis: Can we use organic-rich shales to interpret the tectonic evolution of a depositional basin? Earth Sci Rev. 2008;86(1):1–14. doi:10.1016/j.earscirev.2007.07.001.

Lewan MD. Laboratory simulation of petroleum formation. Org Geochem. 1993;. doi:10.1007/978-1-4615-2890-6_18.

Lewan MD. Experiments on the role of water in petroleum formation. Geochim Cosmochim Acta. 1997;61(17):3691–723. doi:10.1016/S0016-7037(97)00176-2.

Lewan MD, Kotarba MJ, Więcław D, et al. Evaluating transition-metal catalysis in gas generation from the Permian Kupfer-schiefer by hydrous pyrolysis. Geochim Cosmochim Acta. 2008;72(16):4069–93. doi:10.1016/j.gca.2008.06.003.

Li B, Meng ZF, Xia B, et al. Hydrocarbon-generating thermal simulation of uranium-bearing minerals. Acta Pet Mineral. 2008;27(01):52–8. doi:10.3969/j.issn.1000-6524.2008.01.007 **(in Chinese)**.

Liu DY, Liu JZ, Peng PA, et al. Carbon isotope kinetics of gaseous hydrocarbons generated from different kinds of vitrinites. Chin Sci Bull. 2004;49(1):72–8. doi:10.1007/BF02890456 **(in Chinese)**.

Liu CY, Zhao HG, Tan CQ, et al. Occurrences of multiple energy mineral deposits and mineralization/reservoiring system in the basin. Oil Gas Geol. 2006;27(2):131–42. doi:10.3321/j.issn:0253-9985.2006.02.001 **(in Chinese)**.

Liu CY, Mao GZ, Qiu XW, et al. Organic-inorganic energy minerals interactions and the accumulation and mineralization in the same sedimentary basins. Chin J Nat. 2013;35(1):47–55. doi:10.3969/j.issn.0253-9608.2013.01.006 **(in Chinese)**.

Lorant F, Prinzhofer A, Behar F, et al. Carbon isotopic and molecular constraints on the formation and the expulsion of thermogenic hydrocarbon gases. Chem Geol. 1998;147(3):249–64. doi:10.1016/S0009-2541(98)00017-5.

Lu HX, Meng ZF, Li B, et al. Effect of uranium substance on hydrocarbon generation from liginite by hydrous pyrolysis. Xinjiang Pet Geol. 2007;28(06):718–20. doi:10.3969/j.issn.1001-3873.2007.06.016 **(in Chinese)**.

Mango FD. Transition metal catalysis in the generation of petroleum: a genetic anomaly in Ordovician oils. Geochim Cosmochim Acta. 1992;56(10):3851–4. doi:10.1016/0016-7037(92)90153-A.

Mango FD, Joe Hightower. The catalytic decomposition of petroleum into natural gas. Geochim Cosmochim Acta. 1997;61(24):5347–50. doi:10.1016/S0016-7037(97)00310-4.

Mao GZ, Liu CY, Liu BQ, et al. Effects of uranium on hydrocarbon generation of low-mature hydrocarbon source rocks containing kerogen type I. J China Univ Pet. 2012a;36(2):172–81. doi:10.3969/j.issn.1673-5005.2012.02.030 **(in Chinese)**.

Mao GZ, Liu CY, Zhang DD, et al. Effects of uranium (type II) on evolution of hydrocarbon generation of source rocks. Acta Geol Sin. 2012b;86(11):1833–40. doi:10.3969/j.issn.0001-5717.2012.11.013 **(in Chinese)**.

Mao GZ, Liu CY, Zhang DD, et al. Effects of uranium on hydrocarbon generation of hydrocarbon source rocks with type-III kerogen. Sci China Earth Sci. 2014;57:1168–79. doi:10.1007/s11430-013-4723-1 **(in Chinese)**.

Mayer LM. Relationships between mineral surfaces and organic carbon concentrations in soils and sediments. Chem Geol. 1994;114(3–4):347–63. doi:10.1016/0009-2541(94)90063-9.

Pan CC, Geng AS, Zhong NN, et al. Kerogen pyrolysis in the presence and absence of water and minerals: amounts and compositions of bitumen and liquid hydrocarbons. Fuel. 2009;88(5):909–19. doi:10.1016/j.fuel.2008.11.024.

Pan CC, Geng AS, Zhong NN, et al. Kerogen pyrolysis in the presence and absence of water and minerals: steranes and triterpenoids. Fuel. 2010;89(2):336–45. doi:10.1016/j.fuel.2009.06.032.

Partin C, Bekker A, Planavsky N, et al. Large-scale fluctuations in PreCambrian atmospheric and oceanic oxygen levels from the record of U in shales. Earth Planet Sci Lett. 2013;369–370(3):284–93. doi:10.1016/j.epsl.2013.03.031.

Reeves EP, Seewald JS, Sylva SP. Hydrogen isotope exchange between n-alkanes and water under hydrothermal conditions. Geochim Cosmochim Acta. 2012;77:582–99. doi:10.1016/j.gca.2011.10.008.

Schimmelmann A, Lewan MD, Wintsch RP. D/H isotope ratios of kerogen, bitumen, oil, and water in hydrous pyrolysis of source rocks containing kerogen types I, II, IIS, and III. Geochim Cosmochim Acta. 1999;63(22):3751–66. doi:10.1016/S0016-7037(99)00221-5.

Seewald JS. Aqueous geochemistry of low molecular weight hydro-carbons at elevated temperatures and pressures: constraints from mineral buffered laboratory experiments. Geochi Cosmochim

Acta. 2001;65(10):1641–64. doi:10.1016/S0016-7037(01)00544-0.

Seewald JS. Organic-inorganic interactions in petroleum-producing sedimentary basins. Nature. 2003;426(6964):327–33. doi:10.1038/nature02132.

Seewald JS, Benitez-Nelson BC, Whelan Jk. Laboratory and theoretical constraints on the generation and composition of natural gas. Geochim Cosmochim Acta. 1998;62(9):1599–617. doi:10.1016/S0016-7037(98)00000-3.

Sessions AL, Sylva SP, Summons RE, et al. Isotopic exchange of carbon-bound hydrogen over geologic timescales 1. Geochim Cosmochim Acta. 2004;68(7):1545–59. doi:10.1016/j.gca.2003.06.004.

Siskin M, Katritzky AR. Reactivity of organic compounds in hot water: geochemical and technological implications. Science. 1991;254:231–7. doi:10.1126/science.254.5029.231.

Surdam RC, Crossey LJ, Eglinton G, et al. Organic-inorganic reactions during progressive burial: key to porosity and permeability enhancement and preservation [and discussion]. Philos Trans R Soc Lond A Math Phys Eng Sci. 1985;315(315):135–56. doi:10.1098/rsta.1985.0034.

Surdam RC, Jiao ZS, MacGowan DB. Redox reactions involving hydrocarbons and mineral oxidants: a mechanism for significant porosity enhancement in sandstones. AAPG Bull. 1993;77(9):1509–1518.

Sweeney JJ, Burnham AK. Evaluation of a simple model of vitrinite reflectance based on chemical kinetics. AAPG Bull. 1990;74(10):1559–70.

Tang Y, Perry JK, Jenden PD, et al. Mathematical modeling of stable carbon isotope ratios in natural gases. Geochim Cosmochim Acta. 2000;64(15):2673–87. doi:10.1016/S0016-7037(00)00377-X.

Tannenbaum E, Kaplan IR. Low-Mr hydrocarbons generated during hydrous and dry pyrolysis of kerogen. Nature. 1985a;317(6039):708–9. doi:10.1038/317708a0.

Tannenbaum E, Kaplan IR. Role of minerals in the thermal alteration of organic matter - I: Generation of gases and condensates under dry condition. Geochim Cosmochim Acta. 1985b;49(12):2589–604. doi:10.1016/0016-7037(85)90128-0.

Tian H, Xiao XM, Wilkins RW, et al. An experimental comparison of gas generation from three oil fractions: implications for the chemical and stable carbon isotopic signatures of oil cracking gas. Org Geochem. 2012;46:96–112. doi:10.1016/j.orggeochem.2012.01.013.

Xiao XM, Zeng QH, Tian H, et al. Origin and accumulation model of the AK-1 natural gas pool from the Tarim Basin China. Org Geochem. 2005;36(9):1285–98. doi:10.1016/j.orggeochem.2005.04.001.

Xiong YQ, Geng AS, Liu JZ. Kinetic-simulating experiment combined with GC-IRMS analysis: application to identification and assessment of coal-derived methane from Zhongba Gas Field (Sichuan Basin, China). Chem Geol. 2004;213(4):325–38. doi:10.1016/j.chemgeo.2004.07.007.

Zhang T, Ellis GS, Wang KS, et al. Effect of hydrocarbon type on thermochemical sulfate reduction. Org Geochem. 2007;38(6):897–910. doi:10.1016/j.orggeochem.2007.02.004.

Zhang SC, Mi JK, He K. Synthesis of hydrocarbon gases from four different carbon sources and hydrogen gas using a gold-tube system by Fischer–Tropsch method. Chem Geol. 2013;349–350(4):27–35. doi:10.1016/j.chemgeo.2013.03.016.

Zhang SC, Wang XM, Hammarlund EU, et al. Orbital forcing of climate 1.4 billion years ago. Proc Natl Acad Sci U S A. 2015;112(12):1406–13. doi:10.1073/pnas.1502239112.